

Kriging-based spatial interpolation from measurements for sound level mapping in urban areas

Pierre Aumond^a, Arnaud Can^a, Vivien Mallet^b, Bert De Coensel^c, Carlos Ribeiro^d, Dick Botteldooren^e, Catherine Lavandier^f

^a IFSTTAR, CEREMA, UMRAE, F-44344 Bouguenais, France

^b Inria, Paris Research Center, France

^c ASAsense, Belgium, Also at Waves Research Group, Department of Information Technology, Ghent University, Technologiepark-Zwijnaarde 15, B-9052 Ghent

^d Bruitparif, France

^e Waves Research Group, Department of Information Technology, Ghent University, Technologiepark-Zwijnaarde 15, B-9052 Ghent

^f ETIS, CNRS UMR8051, ENSEA, Université de Cergy-Pontoise, France

Abstract

Network-based sound monitoring systems are deployed in various cities over the world and mobile applications allowing participatory sensing are now common. Nevertheless, the sparseness of the collected measurements, either in space or in time, complicates the production of sound maps. This paper describes the results of a measurement campaign that has been conducted in order to test different spatial interpolation strategies for producing sound maps. Mobile measurements have been performed while walking multiple times in every street of the XIIIth district of Paris. By adaptively constructing a noise map on the basis of these measurements, the role of the density of observations and the performance of four different interpolation strategies is investigated. Ordinary and universal Kriging methods are assessed, as well as the effect of using an alternative definition of the distance between observation locations, which takes the topology of the road network into account. The results show that a high density of observation points is necessary to obtain an interpolated sound map close to the reference map.

Keywords: Kriging; Spatial interpolation; Sound map; Opportunistic measurements

I. Introduction

In this work, we investigated the use of a large amount of in situ measurements and the interpolation of these to construct a sound level map.

The Directive 2002/CE/49 contributed to the development and harmonization of noise prediction models (EC 2002). For making urban sound maps, model-based numerical engineering methods are currently widely used and these methods provide a good compromise between accuracy and computation time (Kephelopoulos et al. 2014). Nevertheless, they have many limitations, and the resulting sound maps neglect the diversity of urban sound environments in terms of both sound sources and sound environment dynamics.

Sound maps based on measurements can help to improve sound mapping (Zambon et al. 2017; Asensio 2017; Hong and Jeon 2017; Harman, Koseoglu, and Yigit 2016). The recent development of small and autonomous acoustic sensors contributes to this movement, and network-based sound monitoring systems are being deployed in an increasing number of cities over the world, using either high-quality or low-cost microphones (Mydlarz, Salamon, and Bello 2017; Asensio 2017; Sevillano et al. 2016). Also, smartphone applications, allowing participatory sensing, are now common, which multiplies the amount of available

data to potentially map the sound environment of a city based on measurements (Aspuru et al. 2016; Guillaume et al. 2016; Maisonneuve et al. 2009; Issarny et al. 2016).

Nevertheless, the production of sound maps based on measurements is complicated by metrological issues inherent to the typical microphones used in consumer electronics, the time sparseness of the measurements collected through mobile monitoring applications, and the space sparseness of the measurements collected through fixed sound monitoring networks. Therefore, it is fundamental to know the time and space representativeness of such measurements, as this knowledge is required to be able to propose relevant interpolation methods that can be used to produce sound maps that cover the full temporal and spatial extent of the study area.

The temporal structure of urban sound levels (highly correlated day or week patterns, seasonal trends) can be exploited to restrict the number of sampled days, or to rely only on measurements performed at selected periods of the day, in order to estimate L_{den} values or Daily Average Noise Patterns (Hong and Jeon 2017; Geraghty and O'Mahony 2016; J. M. Barrigón Morillas and Prieto Gajardo 2014; Zuo et al. 2014). Previous studies also revealed that a 10 or 15-minute measurement is representative of a 1h-period in an urban context, as the majority of the 10 or 15 minute-measurements are in the same sound level range during homogeneous periods (Brocolini et al. 2013; Prieto Gajardo and Barrigón Morillas 2015). Other studies that rely on short-term recording methods proved the relevance of 15-minute sampling periods (Morillas et al. 2005; Arnaud Can et al. 2011). Even shorter measurement periods can be found in the literature, especially in those cases where the opportunistic measurement context offered by smartphone applications is used. In this case, the short measurement duration is compensated by the large number of measurements (Guillaume et al. 2016), shifting the focus from the duration of each measurement episode to the number of sampling episodes, as recommended in (Mateus, Dias Carrilho, and Gameiro da Silva 2015).

Zuo et al. (Zuo et al. 2014) showed that the sound level variability in urban environments can be explained for a large part by the spatial characteristics of the environment. Also, the space representativeness and the spatial interpolation of the measurements is an important issue when computing sound maps based on measurements. Maps interpolated from the data obtained through fixed sound measurement stations have recently been produced (Liu et al. 2013; Harman, Koseoglu, and Yigit 2016; Segura Garcia et al. 2016; Huang et al. 2017), and form a useful tool to estimate the noisiness of a neighborhood or to give a global overview of the city sound levels. However, the large distance between measurement stations often does not allow one to map sound levels in each street, which is offered by maps calculated using model-based numerical methods. A study by Can et al. (A. Can, Dekoninck, and Botteldooren 2014) that involved mobile measurements performed using sound level meters attached to backpacks permitted one to compare an interpolated map with a reference map, but only for a very small area (four streets). More studies are therefore needed to investigate the density of measurements that is required to have an acceptable accuracy at the street resolution.

Another parameter to take into account is the method of interpolation. Several methods have been tested for urban sound level interpolation: Inverse Distance Weighting (IDW) methods (A. Can, Dekoninck, and Botteldooren 2014; Harman, Koseoglu, and Yigit 2016; Segura Garcia et al. 2016; Hong and Jeon 2017), Kriging methods (Harman, Koseoglu, and Yigit 2016; A. Can, Dekoninck, and Botteldooren 2014; Segura Garcia et al. 2016) and multiquadratic interpolation (Harman, Koseoglu, and Yigit 2016). Alternative interpolation methods that involve a modified definition of the distance between

measurement locations, in order to account for the city geometry or the road network, have recently been proposed (A. Can, Dekoninck, and Botteldooren 2014; López-Quílez and Muñoz 2009; Hachem et al. 2015). Nevertheless, these interpolation methods have only been tested on small measurement samples, and larger studies are needed to validate the conclusions of these works. It is worth mentioning that the density of measurements appears to be more important than the method of interpolation (Harman, Koseoglu, and Yigit 2016).

Recently, a number of data fusion techniques have been proposed to correct model-based numerically computed sound maps with measurements (Hachem et al. 2015; Wei et al. 2016; Zambon et al. 2017; Ventura et al. 2017). These techniques are promising, but require a pre-calculated sound map, which can be expensive, and give priority to the potential indicators available in this sound map. Most of the existing sound maps involve the energy-equivalent sound level, whereas in situ measurements allow calculating a wide range of acoustical indicators, which may include information about the temporal dynamics of the sound environment; for example, percentile or emergence indicators can also be interesting to interpolate. The spatial interpolation methods can even be based on perceptual assessments (Aletta and Kang 2015).

In this study, a large measurement campaign has been conducted in the XIIIth district of Paris, with the goal to test different spatial interpolation strategies. Mobile measurements have been performed with sound measurement stations attached to backpacks that were carried by researchers when walking in every street of the district between 1 and 15 times. The measurements are aggregated over a grid of locations in the study area, and are used to compute a reference map of the district. An analysis of the sensitivity of the sound level values with respect to the radius of the integration and the number of measurements is done via a bootstrap method. From the reference sound map, four Kriging methods for interpolation between a set of measurement locations are tested, based on a combination of two strategies: (i) Ordinary Kriging and universal Kriging which consists of adding a linear trend, defined from the distance between an observation location of the domain and its closest categorized road, and (ii) a variation of the distance definition between observation locations, which can be Euclidian or computed from the road network to take into account the influence of the city geometry. By progressively decreasing the number of observation locations, the impact of the density of observation locations and the performance of different spatial interpolation methods is investigated.

II. Method

A. Study area

Figure 1 presents the study area, which corresponds to the XIIIth District of Paris. This district includes a large variety of urban sound environments: large avenues with high traffic density, lively streets with bars and restaurants, schools, small and large parks, quiet streets. The size of the study area is approximately 2.8 km² with a maximum extent of 2 km west to east and a maximum extent of 1.7 km north to south.

B. Measurement set-up

All measurements were carried out using dedicated mobile sound measurement stations developed by ASAsense (De Coensel et al. 2015). These stations record the instantaneous 1/3-octave band spectrum with a 125-ms temporal resolution as well as the instantaneous GPS position with a 1-s temporal

121 resolution. Both sound and GPS data are synchronized, such that the spatio-temporal evolution of the
122 sound spectrum during each measurement session can be reconstructed afterwards. In order to fully
123 capture the characteristics of the sound environment, a large set of indicators is calculated on the basis of
124 this 1/3-octave band spectrum data, including the A-weighted energy-equivalent sound level at each
125 second, $L_{eq,1s}$, which is used throughout this study.

126 C. *Mobile measurements*

127 The sound measurement stations were mounted in backpacks with power provided by a battery pack,
128 and, subsequently, mobile measurements were carried out between October 22th 2014 and May 26th 2015.
129 Five operators participated in the measurements. In order to minimize the variation between measurement
130 sessions and to be able to calculate sound levels that are representative for homogeneous sound
131 environments, measurements were only carried out on weekdays, either between 10 a.m. and 12 a.m., or
132 between 2 p.m. and 4 p.m. As shown in (Prieto Gajardo and Barrigón Morillas 2015; Zuo et al. 2014;
133 Brocolini et al. 2013), these periods, which exclude rush hour traffic and lunch times, provide a similar
134 sound environment. Depending on the variability of the sound environment, the number of walks in each
135 street was varied. As shown in (Prieto Gajardo and Barrigón Morillas 2015), the sound environment of a
136 calm street is more sensitive to single sound events than that of a large boulevard, thus a higher number of
137 measurements is required to calculate a sound level value that is representative of the sound environment
138 of a calm street, as compared to a large boulevard. After each day of measurements, the variance of the
139 sound level was computed for each street, providing feedback on those streets that would benefit from
140 more measurements to get a stable estimate. The number of passages per street ranged from 1 to 15 times,
141 with an average of 4 and a standard deviation of 2.7 passages. Figure 1 shows the number of walks (only
142 validated measurements were kept to plot this figure).

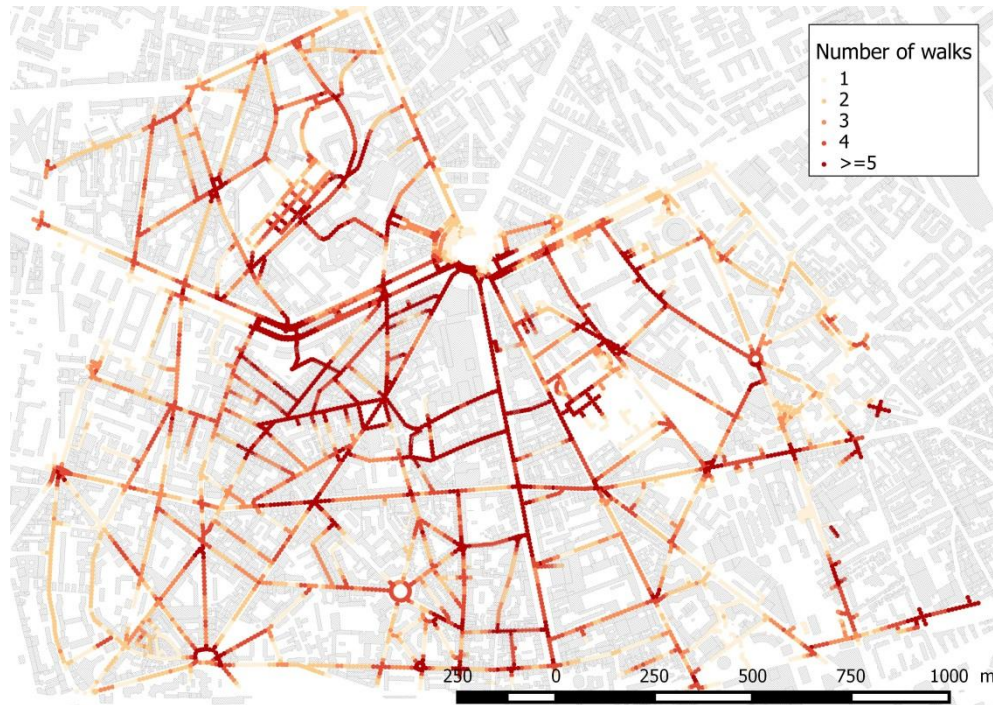


Figure 1 (color online) Number of passages at each location (only validated measurements).

D. Map matching

A GPS track is associated with each measurement session. However, the accuracy of the GPS data depends on many factors such as the quality of the GPS receiver, the characteristics of the surroundings such as the presence of high buildings, or the weather. In this study, the median standard deviation associated with the GPS locations was about 10 meters. Although rarely considered in studies dealing with geo-referenced mobile measurements, this can be problematic for the present analysis, because some measurements can be associated with an erroneous street.

Therefore, it was necessary to preprocess the GPS data, mapping each measurement to a location on the road, a problem commonly known as map-matching. For this study, a point-to-point method was developed, on the basis of the following conditions: (i) all measurements were performed on sidewalks or on roads, and the sound levels measured on both sides of each street are considered to be equivalent and are snapped to the middle of the street; (ii) all GPS locations are snapped to the center of the closest street under the conditions that the operator walked with a maximum speed of 5 km/h and that the map-matched point conserves the same direction of displacement (with a direction tolerance of 60°) as the original point; and (iii) the map-matched points are located at a maximum distance from the original GPS points equal to twice the standard deviation of the GPS tracker.

E. From mobile measurements to observation locations

In a previous study (Aumond et al. 2017), it was shown that the median sound level L_{50} is well correlated with the perceived loudness of an urban sound environment. The median sound level presents

the advantage that it is less sensitive to peaks in the measurement than the energy-equivalent level. Exceptionally, peaks can be generated by the operators themselves, or can occur when extremely noisy vehicles pass by in the vicinity of the operators. In addition, the median sound level L_{50} does not include A-weighting, which is known to reduce too much the influence of low frequencies [63-500 Hz] at sound levels encountered in urban environments, and thus the influence of road traffic sound on overall perceived loudness. The first step in carrying out the spatial interpolation between measurement locations, was to aggregate, at each location, all mobile measurements that are within a radius r . This aggregation step is performed using the median sound level of all the 1-s values $L_{eq,1s}$ considered as independent observations. The associated value is assumed to be representative of the L_{50} sound level at the observation location on weekdays and during the measurement periods [10-12h; 14-16h]. Every aggregated observation location is situated on the road network, because mobile measurements were only taken on sidewalks and pedestrian walkways in the public space. The road network that was used for map-matching was based on OpenStreetMap ("OpenStreetMap" n.d.).

F. Variogram and Kriging

1. Kriging method

Ordinary Kriging method is a well-known interpolation method that has been used in various applications, especially in environmental applications. It also bears similarities with classical data assimilation methods that have helped environmental forecasting, including at urban scale for air pollution (Tilloy et al. 2013) and noise pollution (Ventura et al. 2017; Harman, Koseoglu, and Yigit 2016). The approach is likely to succeed when some meaningful function can fit the empirical variogram, which is the case in this study. Nonetheless, at urban scale, the sound levels exhibit a special distribution due to the city geometry, and this is a difference with typical applications of Kriging (López-Quílez and Muñoz 2009). This is the reason why, in the construction of the variogram, we made use of the distance along the road network instead of a raw Euclidean distance (see Section II.F.3). Also, since it is known that sound levels can be approximated from external data (Juan Miguel Barrigón Morillas et al. 2011) and can provide some sort of prior for the spatial distribution of the sound levels, we also tested universal Kriging, which carries out the interpolation of the measurements on top of a prior sound level map (see Section II.F.4).

2. Implementations and parameters

The variogram and Kriging algorithms presented in this study are applied using the functions `variog` (computation of the variogram), `variofit` (best fit of the variogram) and `krige.conv` (Kriging function) of the packages `GeoR` ("GeoR: Analysis of Geostatistical Data Version 1.7-5.2 from CRAN" n.d.) and `GeoRcb` (López-Quílez and Muñoz 2009). The empirical variogram is computed over a distance of 1000 meters. The classical estimator is chosen to compute the empirical variogram as defined in (Cressie 2015). The Matérn covariance model, as defined in (Diggle and Ribeiro 2007), is used to compute the best fit of the experimental variogram with a fixed value for the shape parameter $\kappa=0.5$ and ϕ the value of the range parameter to estimate.

3. Euclidian vs cost-based distance

The package `GeoR` has been used to interpolate using the Euclidian distance (EUCL). The package `GeoRcb` permits the use of alternative definitions of distance. In this study, the distance between two observation locations has also been defined along the road network as presented in Figure 2. The error correlations in the traffic flow are assumed to be better modeled as a function of the distance along the

road than the Euclidean distance. As a consequence, the use of the distance along the road network presumably allows one to better model errors that come from the traffic. The distance between all the possible observation locations of the domain has been calculated with the Johnson's algorithm of the “distances” function of the package “igraph” of the R software described in (West 2001).

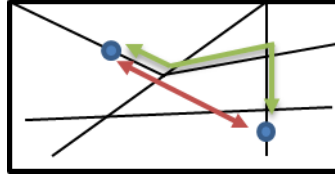


Figure 2(color online) Schema of the road network (shown in black), with the Euclidian Distance (shown in red) as well as the Road Network Distance (shown in green).

4. Ordinary and universal Kriging

Two Kriging methods are compared: Ordinary Kriging (OK) and Universal Kriging (UK). Universal Kriging is a variant of the ordinary Kriging operation that includes a linear trend. Barrigon et al. showed that urban sound is strongly stratified (Morillas et al. 2005). Based on a similar statement, the linear trend T in this study is defined as a linear regression based on 4 explanatory variables which are the distances D_i between the observation locations of the study area and its closest roads belonging to 4 categories i . Equation 1 presents the equation of the trend:

$$T \sim a.D_1 + b.D_2 + c.D_3 + d.D_4 + e$$

in which a , b , c , d and e are adjusted constants.

Road categories have been defined based on the OpenStreetMap attributes as shown in Table 1. Figure 3 presents a map of the study area, in which the roads are shown in different colors according to their category. The first three categories correspond to streets with vehicular traffic, the last one to pedestrian streets.

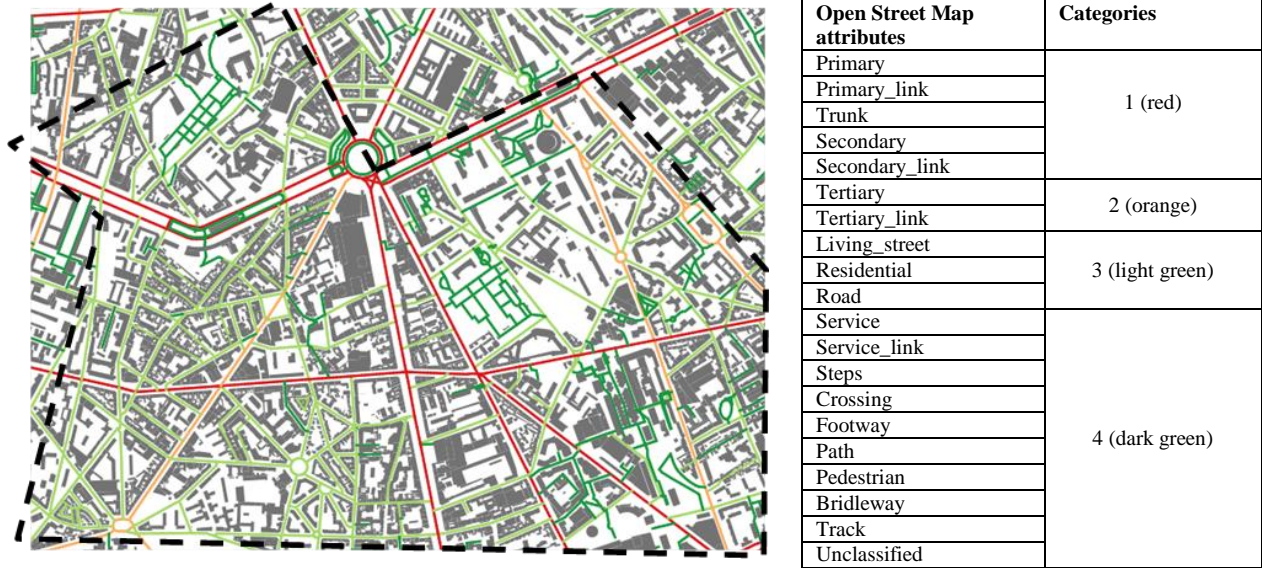


Figure 3 (color online) Outline of the study area (black dashed line) and, in color, the 4 roads categories.

G. Performance metrics

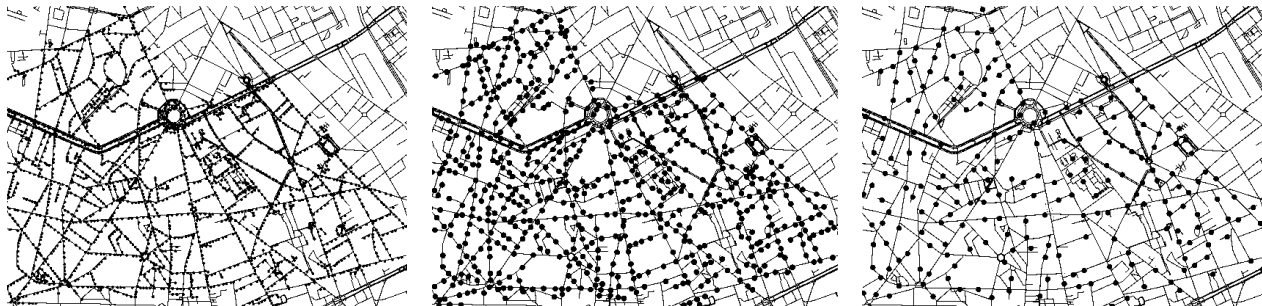
The performance of the interpolation methods is assessed with two indicators: the Root Mean Square Error (RMSE) and the Pearson correlation coefficient (r) between the interpolated and the reference map. The geospatial interpolations are proposed following four methods: (a) ordinary Kriging (OK + EUCL), (b) ordinary Kriging using the distance along the road network (OK + ROAD), (c) universal Kriging (UK + EUCL), (d) universal Kriging using the distance along the road network (UK + ROAD).

III. Results

A. Reference sound map

A reference sound map based on all mobile measurements is first computed. For each observation location, the mobile measurements that are within a specific integration radius are mapped to this location. A sensitivity analysis of the spatial representativeness and the expected accuracy of the sound level at the aggregation radius and the aggregated number of 1-s samples is then performed.

Six values for the aggregation radius have been tested: 2.5 m, 5 m, 10 m, 15 m, 25 m and 50 m. For each radius value, a set of observation locations has been selected, uniformly distributed. For this statistical analysis, the observation locations are spaced apart by at least two times the radius value, to avoid redundancy. In Figure 4, three of those subsets of observation locations are shown.



(a) (b) (c)
Figure 4 Example of three selected sets of observation locations (dots) for radii: (a) 2.5m, (b) 15 m and (c) 50m. Observation locations are located on the study area road network (solid lines).

Figure 5(a) shows the distribution of the aggregated sound levels L_{50} over the study area for the smallest and largest aggregation radii (2.5m and 50m) as presented in Section II.E. Figure 5 (b) shows the $P_{90}-P_{10}$ indicator (where P_{10} and P_{90} are the percentiles 10 and 90 of the sound level distributions), which reflects the width of these distributions for all the studied aggregation radii. As expected, the range of the aggregated sound levels L_{50} over the study area decreases as the value of the radius increases. More prosaically, the reference sound map will appear to be blurred. A small radius will give rise to a more detailed reference sound map, but comes with a decreased number of measurements at each location that may therefore no longer be representative. The results show that the influence of the aggregation radius over the sound level distribution is relatively small, with $P_{90}-P_{10}$ decreasing from 13.5 dB to 10.5 dB.

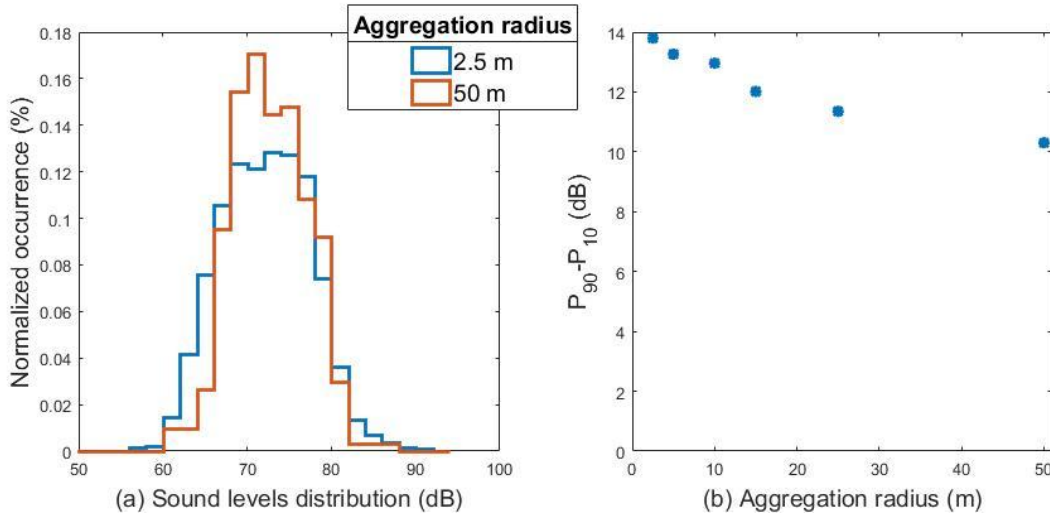


Figure 5 (color online) (a) Distribution of the aggregated sound levels L_{50} over the study area for two values of the aggregation radius. (b) Width of the distribution of the sound levels ($P_{90}-P_{10}$) for 6 different aggregation radii

A bootstrapping method (bootstrap function, statistical toolbox, Matlab) is proposed to analyze the sensitivity of the L_{50} value to the aggregation radius and the number of measurements. This method relies on random sampling, with replacement, of the 1-s measurements for each location within the study area (Efron 1979). Multiple replications of the method permits the computation of the variance associated with the average L_{50} value at each observation location due to the sample characteristics. Figure 6 presents (a) the standard deviation of 1000 bootstrap replications of the calculated L_{50} varying with the number of 1-s samples and (b) the relationship between the aggregation radius and the proportion of retained locations, considering a minimum number of 1-second samples of 180. The correlation between these two parameters is statistically significant ($r=0.53$, $p<.05$), but a large aggregation radius does not always imply a large number of measurements (e.g., along the borders of the study area) and vice versa (e.g., if the operator measured a few minutes at one specific location).

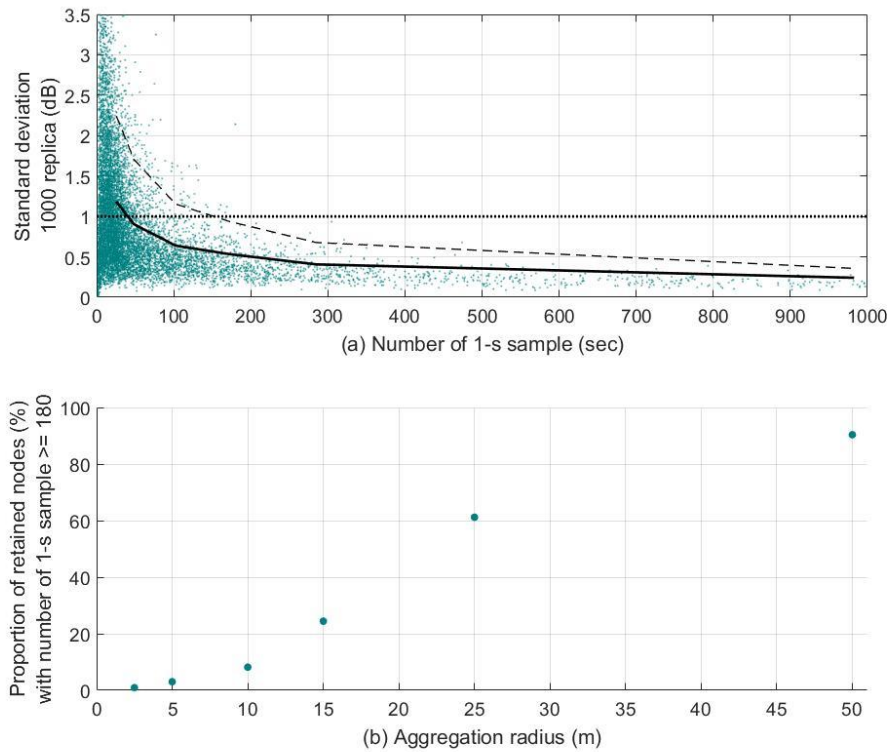


Figure 6 (color online) The upper plot shows the relationship between the standard deviation of 1000 replications (subsets) of the underlying reference data set and the number of 1-s samples of the subsets. The lower plot shows the relationship between the aggregation radius and the proportion of retained measurement locations, considering a minimum number of 1-second samples of 180. Each dot represents a replication, the solid line denotes the mean value, the dashed line denotes the percentile-90).

The variation specific to each location is found to be considerably smaller than the global variation between the locations over the whole study area, which is about 5 dB (see Figure 5). If we consider a standard deviation smaller than 1 dB as acceptable, 90% of the calculated standard deviations are below this threshold when a sample is composed by a minimum of 180 1-s measurements. The chosen threshold also guarantees to have enough data to carry out the spatial analysis. An aggregation radius of 25 meters is chosen as the threshold value because it permits one to retain more than 60% of the computed locations. This aggregation radius also has the advantage that it corresponds to the longitudinal spatial representativeness of sound level measurements found in literature, perceptually (Brocolini et al. 2009) or physically (A. Can, Dekoninck, and Botteldooren 2014), thus suggesting that the resulting sound level map will be consistent with observed spatio-temporal variations.

On the basis of the above results, it can be concluded that, at least for the urban study area considered, three-minute measurements provide sufficient confidence in the aggregated measurement value, even if its representativeness is not guaranteed. As the purpose of the present study was to perform a comparison of interpolation techniques, the calculated sound maps only need to respect the spatial variation of the sound level, but do not necessarily need to be representative of a homogeneous time period.

Figure 7 presents the resulting reference map of the median sound level (L_{50} , dB). For the calculation of this map, a distance of 10 m between each observation location was used, resulting in 4360 locations.

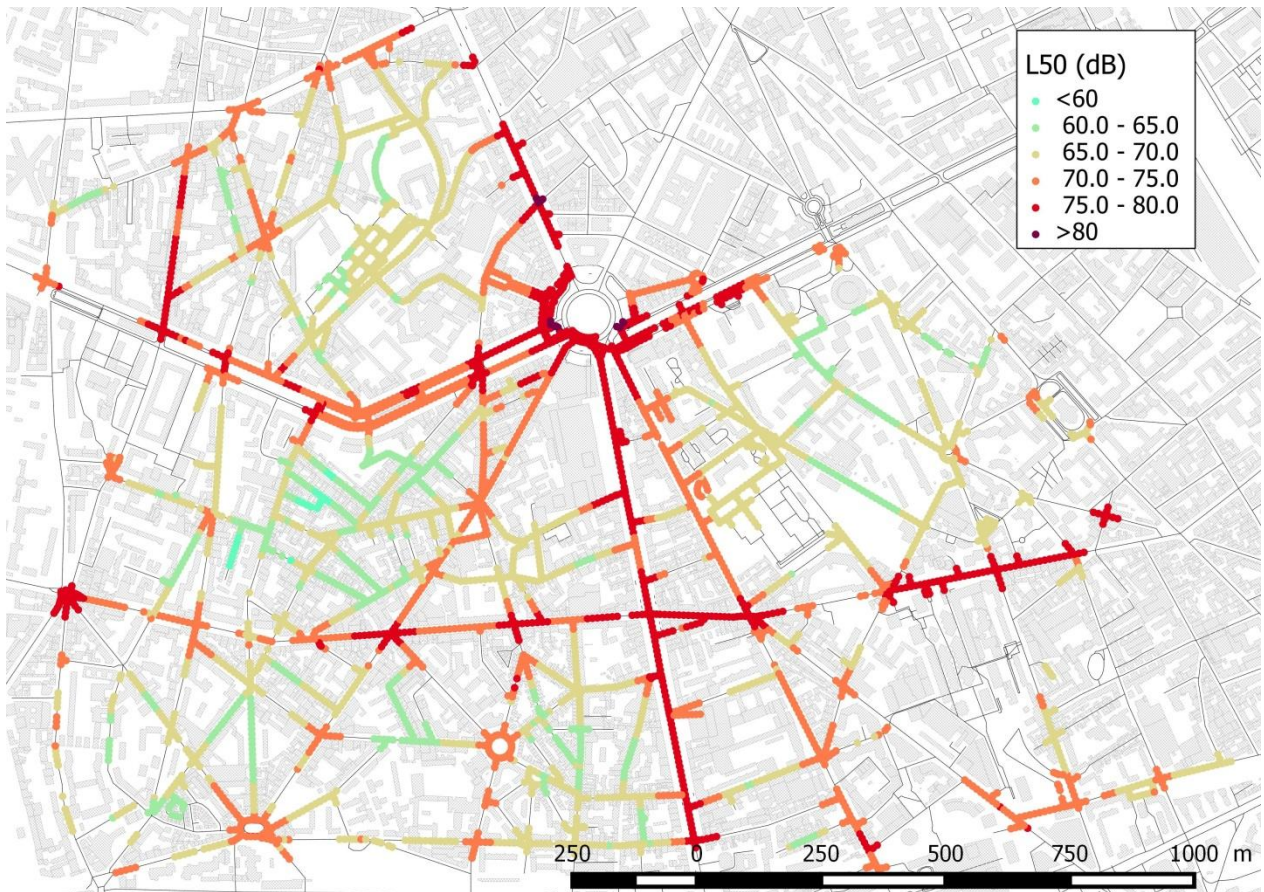


Figure 7 (color online) Reference sound map, integration radius 25 meters, integration time > 180 sec. (n= 4360)

B. Spatial dependence of the data

The spatial dependence of the data is highlighted through the calculation of variograms, which express the semivariance between L_{50} values for a couple of locations according to their distance. On Figure 8, four fitted variograms derived from the reference sound map are presented: (a) an ordinary variogram with the Euclidean distance (OK+EUCL), (b) an ordinary variogram using the distance along the road network (OK+ROAD) (c) an universal variogram which accounts for the trend with the Euclidean distance (UK+EUCL), (d) an universal variogram which accounts for the trend and also uses the distance along the road network (UK+ROAD).

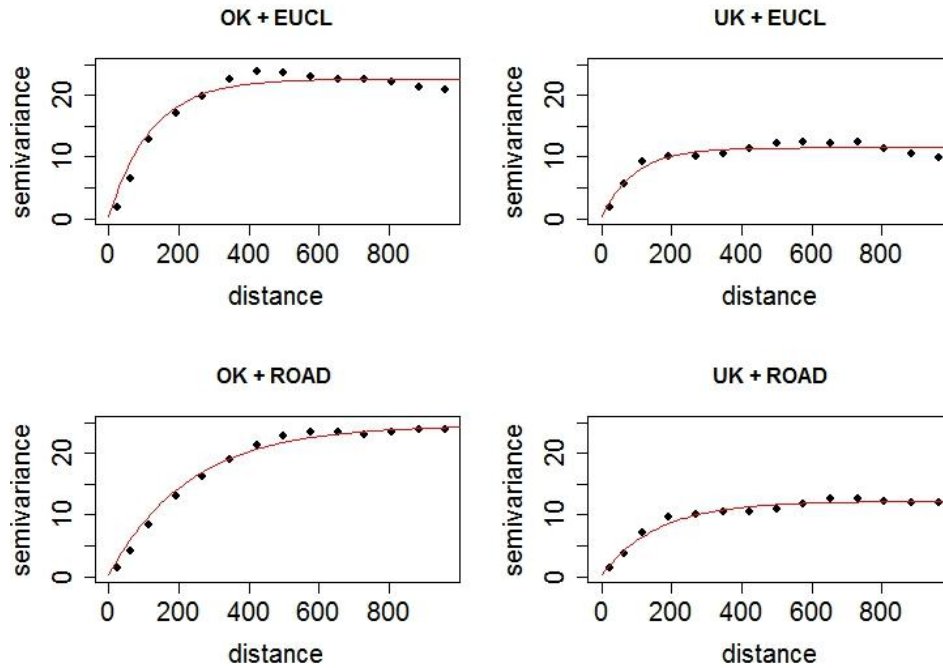


Figure 8 Empirical variograms (dots) and best fitted parametrical models (red line) computed using the ordinary Kriging (OK) and universal Kriging (UK) methods. The printed distance is computed using the Euclidian distance (EUCL) or the distance along the road network (ROAD) (distance in meters, and semivariance in dB²).

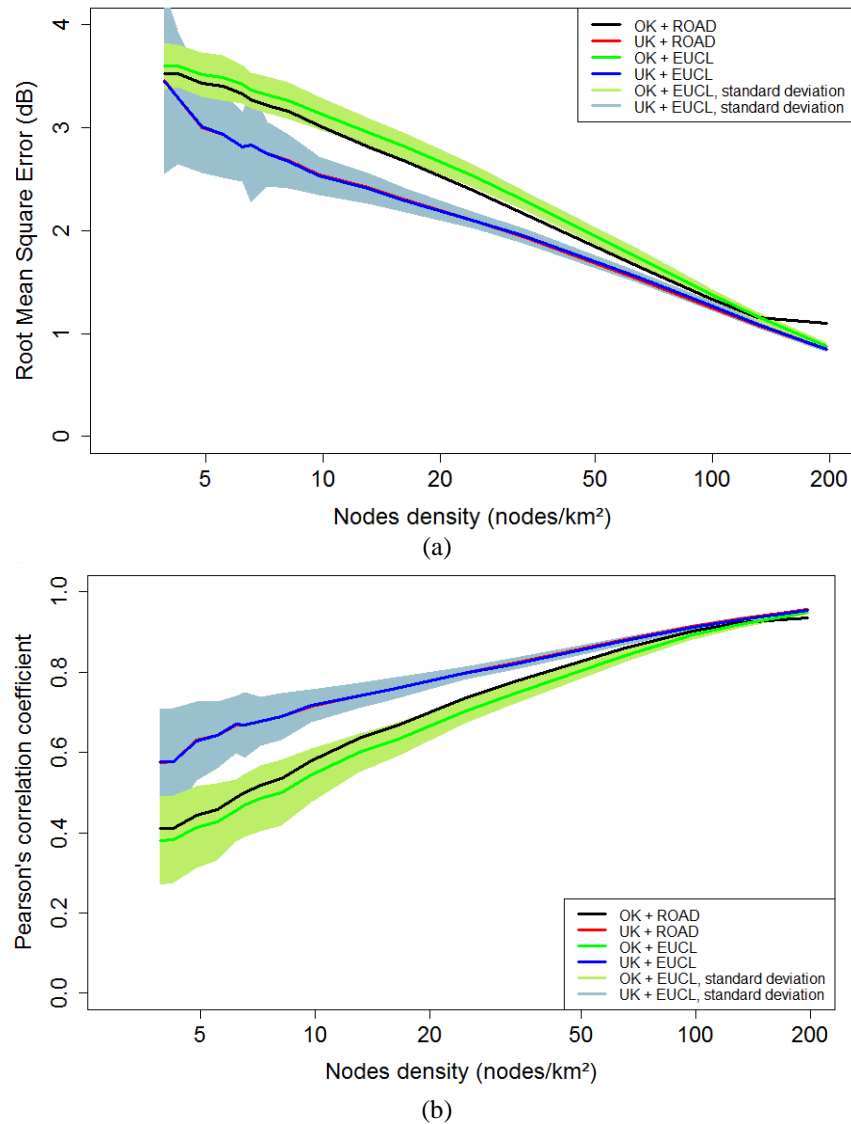
The parameters of the best fitted covariance models are presented in Table 1. The practical ranges of the variograms, defined as the value for which the correlation function decays to 5% of its value at 0, are (a) 366 m for OK+EUCL (b) 285 m for UK+EUCL (c) 691 m for OK+ ROAD (d) 481 m for UK+ROAD. For OK+EUCL, hardly any information is given by an observation to an estimated value located in a radius superior to 366 m. As the nugget variance τ^2 is null, the variogram asymptote, or sill value, corresponds to the signal variance σ^2 . This value at 1000 meters is 22.4 dB² and 24.2 dB² for OK + EUCL and OK + ROAD methods, and 11.2 dB² and 11.9 dB² for UK + EUCL and UK + ROAD. Thus, adding the trend permits one to considerably reduce the signal variance and illustrates the strong correlation between the urban sound levels and the proximity to different types of roads. Also, the practical range of the variograms increases when the alternative definition of distance from the road network is used (from 366 to 691 m and from 285 to 481 m).

Table 1 – Parameters of the Kriging methods

Kriging method	Covariance model	Nugget variance (dB²) τ^2	Sill (dB²) σ^2	Range parameter (m) ϕ	Practical Range (m)
OK+EUCL	Matérn with fixed $\kappa = 0.5$	0	22.4	122.2	366
UK+EUCL	Matérn with fixed $\kappa = 0.5$	0	11.2	95.1	285
OK+ROAD	Matérn with fixed $\kappa = 0.5$	0	24.2	230.7	691
UK+ROAD	Matérn with fixed $\kappa = 0.5$	0	11.9	160.6	481

322 C. *Spatial interpolation and performance analysis*

323 A subset of the observation locations is selected from the reference map and is interpolated over the
 324 whole study area using the four tested strategies. As described in Section III.A, the median sound level
 325 values at the observation locations are computed from at least 180 $L_{eq,1s}$ measurements included in a 25 m
 326 radius around each observation location. The subset of observation locations for evaluation is randomly
 327 selected and 1000 replications are performed for each subset configuration. The replications give
 328 information about the variability due to a chosen set of observation nodes. Figure 9 presents the
 329 relationships between two indicators of performance (RMSE and the Pearson correlation coefficient), and
 330 the density of nodes (number of nodes per sq. km) for the four methods of interpolation.



331 Figure 9 (color online) Relationships between the two indicators of quality (RMSE and the Pearson correlation coefficient), and the density of
 332 nodes (number of nodes per sq. km) for the four methods of interpolation. The area corresponds to the standard deviation associated with the 1000
 333 replications. (The red and blue lines are nearly superposed).
 334

Universal Kriging (UK) considerably increases the quality of the results on both indicators compared to ordinary Kriging (OK). Taking into account the distance along the road network (ROAD) only leads to better results for the ordinary Kriging cases.

From a practical point of view, in case only fixed measurement stations are used, 15 observation locations per sq. km is already a large number. In this case, Figure 9 shows that the correlation between interpolated and reference sound levels is between 0.5 and 0.8, and that the RMSE value is between 2.5 and 3.5 dB. Figure 10 shows an interpolated sound map, using the UK + EUCL and the OK + EUCL methods, based on one of the random sets of 42 observation locations (15 locations per sq. km). The associated prediction standard error maps are also given, as the Kriging methods give access to this information (Diggle and Ribeiro 2007). Figure 10 shows a good correspondence with the reference sound map (see Figure 7). Nevertheless, the dispersion in Figure 9 shows that the observation locations have an important influence over the performance of the algorithm.

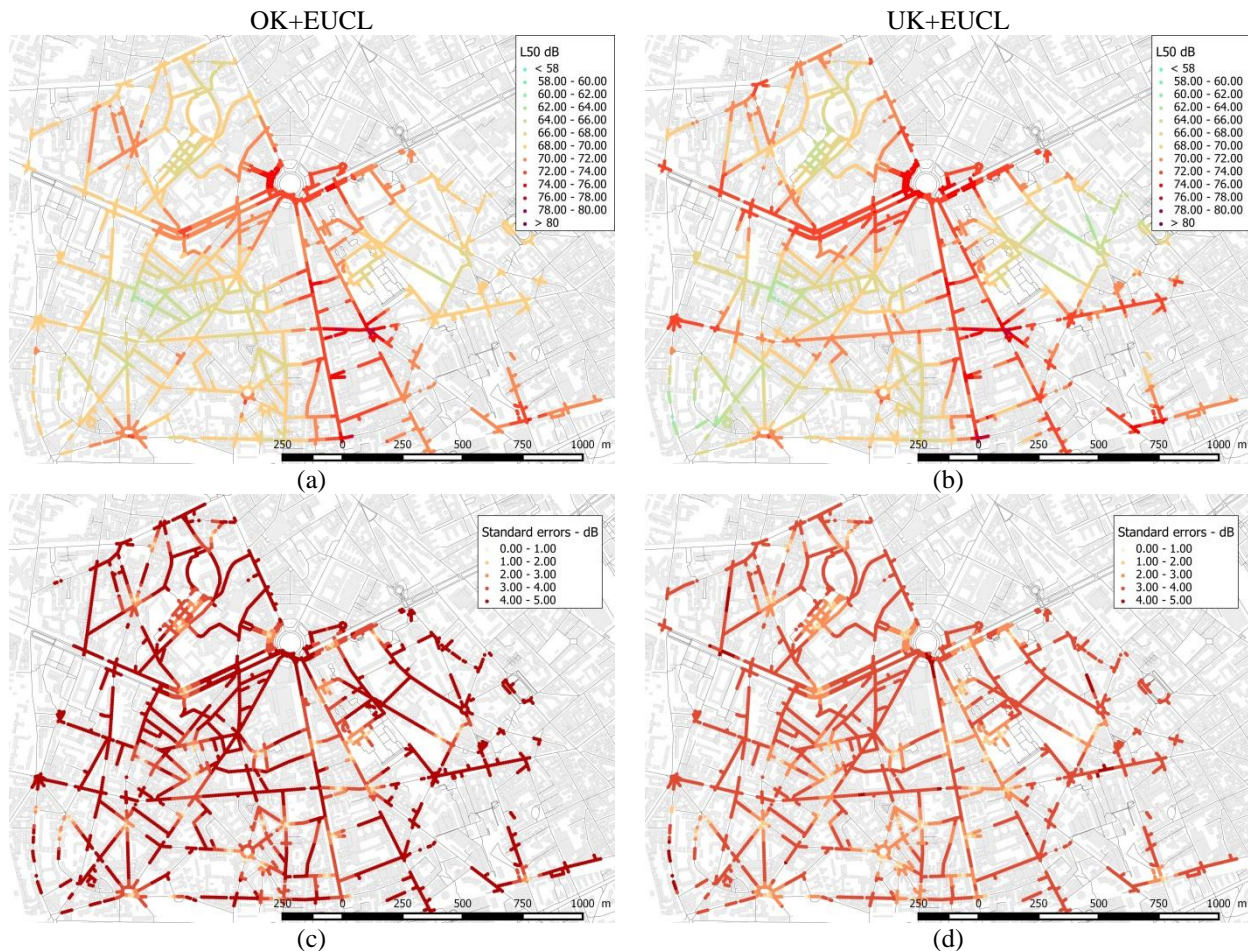


Figure 10 (color online) Example of an interpolated sound map from 42 observations: Estimated L_{50} values using the (a) OK+EUCL and (b) UK+EUCL Kriging methods, and the associated standard errors maps (c) OK+EUCL and (d) UK+EUCL

Figure 11 shows the average errors for the 1000 replications (42 observation locations), against the reference map presented in Figure 7. Figure 11 (a-d) shows that all the interpolation strategies

underestimate the sound level for large boulevards and overestimate the sound level for quiet places, but this is a common limitation of interpolation methods. This is less pronounced for universal Kriging (Figure 11 (b), Figure 11 (d)). In this case, the trend partly corrects this shortcoming, and the errors are distributed more uniformly over the study area. A comparison between Figure 11(a) and (c) or Figure 11(b) and (d) shows the difference between the use of the Euclidian and the road network distance; no major influence is observable.

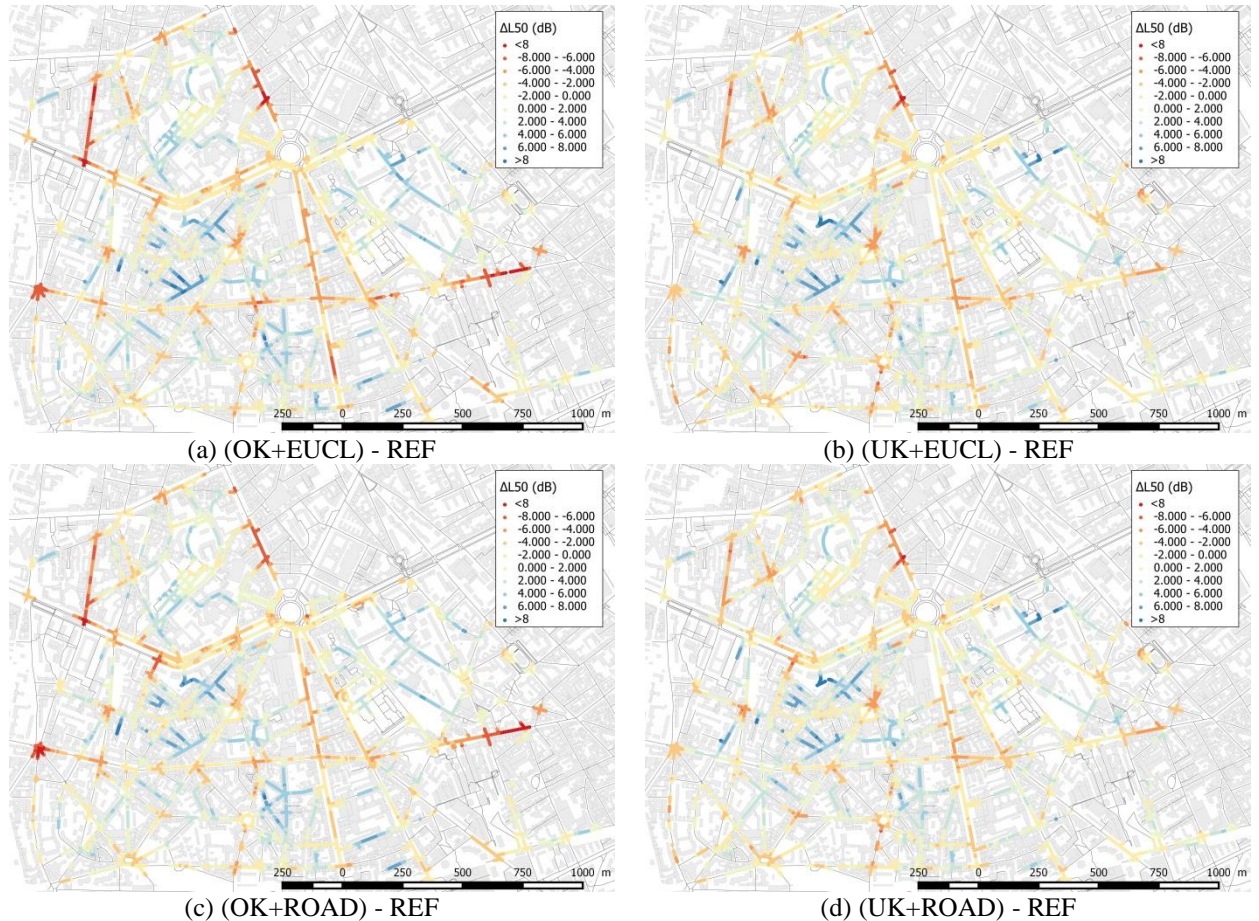


Figure 11 (color online) Average errors for 1000 replications (42 observation locations) against the reference map REF for the four interpolation methods (a) OK+EUCL, (b) UK+EUCL, (c) OK+ROAD and (d) UK+ROAD.

Figure 9 shows that the standard deviation of the performance indicators can be important, especially in case of a small density of measurement locations. In order to identify the principal factors which influence the performance of the Kriging algorithms, a short statistical analysis has been performed over geospatial indicators of the spatial distribution of 42 observations. Table 2 presents some of the parameters which have been calculated for each generated set of observations.

The Variance Mean Ratio (VMR), also called index of dispersion, is an indicator of a good dispersion of the observations over the domain. For this, the domain is divided in 6x6 cells. In each cell, the number of observations is calculated. The variance mean ratio corresponds to the ratio between (i) the variance of the number of observations between each cell, and (ii) the mean number of observations for a cell. If VMR is equal to 1, the observations are randomly dispersed; if $VMR < 1$ the observations are more

dispersed than random (*e.g.*, regular distribution); if $VMR > 1$ the observations are more clustered than a random dispersion.

MEAN_ROAD, STD_ROAD, KURT_ROAD, SKEW_ROAD are indicators of the distribution of the observations over the road categories (integers from 1 to 4, see Figure 2). For example, if MEAN_ROAD is equal to 1 and STD_ROAD equal to 0, it means that all the observations are located over roads of type 1 (avenue/boulevard).

Finally, the CENTER indicator represents the distance between the center of gravity of the observation locations and the center of gravity of the whole road network within the case study area. If CENTER is small, the observations are well centered over the domain.

Table 2 – Geospatial indicators of the observation locations.

Index	Name	Range
VMR	Variance Mean Ratio	[0.8 – 1.9]
STD_L50	Standard deviation on observed sound levels (L_{50})	[2.8– 6] (dB)
MEAN_ROAD	Average closest road categories	[1.7 – 2.8]
STD_ROAD	Standard deviation on closest road categories	[0.5 – 1.2]
KURT_ROAD	Kurtosis closest road categories	[-0.19 – 1.6]
SKEW_ROAD	Skewness closest road categories	[1.4 – 7.4]
CENTER	Distance between the gravity center of the observations and the gravity center of the whole network	[0.34 – 364] (m)

Table 3 presents the Pearson correlation coefficient between the spatial distribution indicators and the performance indicators. It shows that the STD_L50 is the only geospatial indicator that is well correlated with the performance indicators, particularly for ordinary Kriging. As it can be expected, this suggests that the measurement stations should be placed in locations that represent a large distribution of sound levels. For universal Kriging, this factor is less important because of the correction brought by the trends. The same analysis was carried out with other performance metrics than the Pearson correlation coefficient, but this did not bring more information.

Table 3 – Pearson correlation coefficient between the geospatial and performance indicators for two Kriging methods (* $p < 0.05$).

	r (OK+EUCL)	r (UK+EUCL)	RMSE (OK+EUCL)	RMSE (UK+EUCL)
VMR	0.06*		-0.07*	
STD_L50	0.48*	0.27*	-0.55*	-0.21*
MEAN_ROAD	0.07*			-0.04*
STD_ROAD	0.19*	0.07*	-0.19*	-0.10*
KURT_ROAD	-0.10*	-0.06*	0.07*	0.09*
SKEW_ROAD	-0.16*	-0.07*	0.14*	0.11*
CENTER	-0.05*		0.06*	

IV. Discussion

As the study area was the XIIIth district of Paris, the variogram and Kriging parameters were only adjusted for this district. Even if some of these parameters are comparable with those from previous studies (A. Can, Dekoninck, and Botteldooren 2014), other replications in other urban contexts will be necessary to extend the conclusions of this work.

On the one hand, the alternative definition of distance along the road network slightly increases the performance of the algorithms, but only for ordinary Kriging methods. On the other hand, the proposed trend based on the distance to the closest roads by category, as defined in Section II.F.4, strongly improves the results for all Kriging methods. These results confirm the observations done in (Morillas et al. 2005; Rey Gozalo, Barrigón Morillas, and Prieto Gajardo 2015; Juan Miguel Barrigón Morillas et al. 2011) which state that using a street categorization method that accounts for street use is particularly appropriate to study the spatial variability of urban sound levels. Thus, to continue to improve the performance of the interpolation methods, efforts should be focused on the trend definition. Nevertheless, a complex trend definition is comparable to the computation of a model-based sound map. Moreover, it might increase the computational cost of the interpolation method considerably, and can possibly introduce new error sources.

The errors associated with the observations are not taken into account in our Kriging approach; nevertheless, a follow-up study should investigate the integration of noisy observations with a proper uncertainty associated with each measurement location. Maybe data assimilation methods used in geosciences, *e.g.*, computing the so-called best linear unbiased method (Bouttier et al. 2002; Tilloy et al. 2013), could be useful to achieve this task.

All the presented results are valid for one homogeneous time period. Time interpolation could be added. This interpolation could be done in pre- or post-processing, relying on previous works dealing with temporal interpolation of urban sound levels (Prieto Gajardo et al. 2016) or directly with a spatio-temporal Kriging.

Finally, this study shows the influence of the spread of observation locations over the study area to correctly interpolate sound levels. As it can be expected, the results suggest that fixed measurement stations should be placed to obtain a large distribution of sound levels and so, a large variety of sound environments. Nevertheless, even if it can be estimated, this information is not fully available prior to the installation of the measurement stations. Other indicators, such as the distribution of the measurement stations over the various road categories, or the location of the center of gravity of the measurement stations, which are available a priori, do not show relevant relationship with performance indicators.

V. Conclusion

By means of a progressive degradation of a reference map of 2.8 km² interpolated from geo-referenced mobile measurements, spatial interpolation methods were compared. The impact of the density of observation points and the performance of four spatial interpolation methods were presented. The four interpolation methods were constructed by combining two algorithms: (i) the Kriging method, either ordinary Kriging or universal Kriging (which consists in adding a linear trend, defined from the distance between each location and its closest road in each category) and (ii) the definition of the distance between locations, either Euclidian or computed from the road network.

The main conclusions are:

- A minimum of 180 1-s measurements are needed to obtain an acceptable level of confidence (1dB) in the L_{50} value calculated at each location within the study area, with an aggregation radius of 25 m.

- The practical ranges of the variograms computed for the four Kriging methods are between 250 and 700 meters.
- Using the distance along the road network in the Kriging method considerably increases the performance in case of ordinary Kriging, but not in case of universal Kriging.
- Universal Kriging, which consists of adding a local trend in the ordinary Kriging formulation, is a promising method. Nevertheless, it introduces an additional calculation of the trend that has a pre-processing cost and can in itself be a source of error.
- Approximately 50 observation locations per sq. km are needed in order to get a correlation coefficient superior to 0.8 and a RMSE value inferior to 2.5 dB between the reference and the interpolated map.

In view of the large density of observation locations needed to obtain a sound map with a high accuracy and the strong improvement brought by the trend in the Kriging formulation, further studies should probably focus on fusion or assimilation techniques combining measurements and numerical simulation results.

Acknowledgments

This work was carried out in the framework of the GRAFIC project, supported by the French Environment and Energy Management Agency (ADEME) under contract No. 1317C0028. The authors also would like to thank the BruitParif team which completed most of the measurements.

References

- Aletta, Francesco, and Jian Kang. 2015. "Soundscape Approach Integrating Noise Mapping Techniques: A Case Study in Brighton, UK." *Noise Mapping* 2 (1): 1–12. <https://doi.org/10.1515/noise-2015-0001>.
- Asensio, César. 2017. "Acoustics in Smart Cities." *Applied Acoustics*, Acoustics in Smart Cities, 117, Part B (February): 191–92. <https://doi.org/10.1016/j.apacoust.2016.11.013>.
- Aspuru, Itziar, Igone García, Karmele Herranz, and Alvaro Santander. 2016. "CITI-SENSE: Methods and Tools for Empowering Citizens to Observe Acoustic Comfort in Outdoor Public Spaces." *Noise Mapping* 3 (1): 37–48. <https://doi.org/10.1515/noise-2016-0003>.
- Aumond, Pierre, Arnaud Can, Bert De Coensel, Dick Botteldooren, Carlos Ribeiro, and Catherine Lavandier. 2017. "Modeling Soundscape Pleasantness Using Perceptual Assessments and Acoustic Measurements Along Paths in Urban Context." *Acta Acustica United with Acustica* 103 (3): 430–43. <https://doi.org/10.3813/AAA.919073>.
- Barrigón Morillas, J. M., and C. Prieto Gajardo. 2014. "Uncertainty Evaluation of Continuous Noise Sampling." *Applied Acoustics* 75 (January): 27–36. <https://doi.org/10.1016/j.apacoust.2013.07.005>.
- Barrigón Morillas, Juan Miguel, Valentín Gómez Escobar, José Trujillo Carmona, Juan Antonio Méndez Sierra, Rosendo Vélchez-Gómez, and Francisco Javier Carmona del Río. 2011. "Analysis of the Prediction Capacity of a Categorization Method for Urban Noise Assessment." *Applied Acoustics* 72 (10): 760–71. <https://doi.org/10.1016/j.apacoust.2011.04.008>.
- Bouttier, F., P. Courtier, P. Courtier, and P. Courtier. 2002. "Data Assimilation Concepts and Methods." 2002.

- Brocolini, Laurent, Catherine Lavandier, Mathias Quoy, and Carlos Ribeiro. 2009. "Discrimination of Urban Soundscape through Kohonen Map." In . Edinburgh, Scotland. <http://publis-etis.ensea.fr/2009/BLQR09/>.
- . 2013. "Measurements of Acoustic Environments for Urban Soundscapes: Choice of Homogeneous Periods, Optimization of Durations, and Selection of Indicators." *The Journal of the Acoustical Society of America* 134 (1): 813–21. <https://doi.org/10.1121/1.4807809>.
- Can, A., L. Dekoninck, and D. Botteldooren. 2014. "Measurement Network for Urban Noise Assessment: Comparison of Mobile Measurements and Spatial Interpolation Approaches." *Applied Acoustics* 83 (September): 32–39. <https://doi.org/10.1016/j.apacoust.2014.03.012>.
- Can, Arnaud, Timothy Van Renterghem, Michael Rademaker, Samuel Dauwe, Pieter Thomas, Bernard De Baets, and Dick Botteldooren. 2011. "Sampling Approaches to Predict Urban Street Noise Levels Using Fixed and Temporary Microphones." *Journal of Environmental Monitoring: JEM* 13 (10): 2710–19. <https://doi.org/10.1039/c1em10292c>.
- Cressie, Noël. 2015. *Statistics for Spatial Data*. Revised Edition. Wiley.
- De Coensel, Bert, Kang Sun, Weigang Wei, Timothy Van Renterghem, Matthieu Sineau, Carlos Ribeiro, Arnaud Can, Pierre Aumond, Catherine Lavandier, and Dick Botteldooren. 2015. "Dynamic Noise Mapping Based on Fixed and Mobile Sound Measurements." In *Euronoise 2015, the 10th European Congress and Exposition on Noise Control Engineering*.
- Diggle, Peter, and Paulo Justiniano Ribeiro. 2007. *Model-Based Geostatistics*. Springer.
- EC. 2002. "Directive 2002/49/EC of the European Parliament and the Council of 25 June 2002 Relating to the Assessment and Management of Environmental Noise." *Official Journal of the European Communities* 189 (12): 12–25.
- Efron, B. 1979. "Bootstrap Methods: Another Look at the Jackknife." *The Annals of Statistics* 7 (1): 1–26. <https://doi.org/10.1214/aos/1176344552>.
- "GeoR: Analysis of Geostatistical Data Version 1.7-5.2 from CRAN." n.d. Accessed May 30, 2017. <https://rdrr.io/cran/geoR/>.
- Geraghty, Dermot, and Margaret O'Mahony. 2016. "Investigating the Temporal Variability of Noise in an Urban Environment." *International Journal of Sustainable Built Environment* 5 (1): 34–45. <https://doi.org/10.1016/j.ijbsbe.2016.01.002>.
- Guillaume, Gwenaël, Arnaud Can, Gwendall Petit, Nicolas Fortin, Sylvain Palominos, Benoit Gauvreau, Erwan Bocher, and Judicaël Picaut. 2016. "Noise Mapping Based on Participative Measurements." *Noise Mapping* 3 (1): 140–56. <https://doi.org/10.1515/noise-2016-0011>.
- Hachem, S., V. Mallet, R. Ventura, A. Pathak, V. Issarny, P. G. Raverdy, and R. Bhatia. 2015. "Monitoring Noise Pollution Using the Urban Civics Middleware." In *2015 IEEE First International Conference on Big Data Computing Service and Applications*, 52–61. <https://doi.org/10.1109/BigDataService.2015.16>.
- Harman, Bilgehan Ilker, Hasan Koseoglu, and Cemal Ozer Yigit. 2016. "Performance Evaluation of IDW, Kriging and Multiquadric Interpolation Methods in Producing Noise Mapping: A Case Study at the City of Isparta, Turkey." *Applied Acoustics* 112 (November): 147–57. <https://doi.org/10.1016/j.apacoust.2016.05.024>.
- Hong, Joo Young, and Jin Yong Jeon. 2017. "Exploring Spatial Relationships among Soundscape Variables in Urban Areas: A Spatial Statistical Modelling Approach." *Landscape and Urban Planning* 157 (January): 352–64. <https://doi.org/10.1016/j.landurbplan.2016.08.006>.
- Huang, Baoxiang, Zhenkuan Pan, Huan Yang, Guojia Hou, and Weibo Wei. 2017. "Optimizing Stations Location for Urban Noise Continuous Intelligent Monitoring." *Applied Acoustics* 127 (December): 250–59. <https://doi.org/10.1016/j.apacoust.2017.06.009>.

- Issarny, Valerie, Vivien Mallet, Kinh Nguyen, Pierre-Guillaume Raverdy, Fadwa Rebhi, and Raphael Ventura. 2016. "Dos and Don'ts in Mobile Phone Sensing Middleware: Learning from a Large-Scale Experiment." In . <https://doi.org/10.1145/2988336.2988353>.
- Kephalopoulos, Stylianos, Marco Paviotti, Fabienne Anfosso-Lédée, Dirk Van Maercke, Simon Shilton, and Nigel Jones. 2014. "Advances in the Development of Common Noise Assessment Methods in Europe: The CNOSSOS-EU Framework for Strategic Environmental Noise Mapping." *The Science of the Total Environment* 482–483 (June): 400–410. <https://doi.org/10.1016/j.scitotenv.2014.02.031>.
- Liu, Jiang, Jian Kang, Tao Luo, Holger Behm, and Timothy Coppack. 2013. "Spatiotemporal Variability of Soundscapes in a Multiple Functional Urban Area." *Landscape and Urban Planning* 115: 1–9. <https://doi.org/10.1016/j.landurbplan.2013.03.008>.
- López-Quílez, Antonio, and Facundo Muñoz. 2009. "Geostatistical Computing of Acoustic Maps in the Presence of Barriers." *Mathematical and Computer Modelling, Mathematical Models in Medicine & Engineering*, 50 (5): 929–38. <https://doi.org/10.1016/j.mcm.2009.05.021>.
- Maisonneuve, Nicolas, Matthias Stevens, Maria E. Niessen, and Luc Steels. 2009. "NoiseTube: Measuring and Mapping Noise Pollution with Mobile Phones." *Environmental Science and Engineering (Subseries: Environmental Science)*, 215–28. <https://doi.org/10.1007/978-3-540-88351-7-16>.
- Mateus, Mário, João A. Dias Carrilho, and Manuel C. Gameiro da Silva. 2015. "Assessing the Influence of the Sampling Strategy on the Uncertainty of Environmental Noise Measurements through the Bootstrap Method." *Applied Acoustics* 89 (Supplement C): 159–65. <https://doi.org/10.1016/j.apacoust.2014.09.021>.
- Morillas, Juan Miguel Barrigón, Valentín Gómez Escobar, Juan Antonio Méndez Sierra, Rosendo Vílchez-Gómez, José M. Vaquero, and José Trujillo Carmona. 2005. "A Categorization Method Applied to the Study of Urban Road Traffic Noise." *The Journal of the Acoustical Society of America* 117 (5): 2844–52.
- Mydlarz, Charlie, Justin Salamon, and Juan Pablo Bello. 2017. "The Implementation of Low-Cost Urban Acoustic Monitoring Devices." *Applied Acoustics, Acoustics in Smart Cities*, 117, Part B (February): 207–18. <https://doi.org/10.1016/j.apacoust.2016.06.010>.
- "OpenStreetMap." n.d. Accessed May 30, 2017. <https://www.openstreetmap.org/#map=16/49.6008/1.1135>.
- Prieto Gajardo, Carlos, and Juan Miguel Barrigón Morillas. 2015. "Stabilisation Patterns of Hourly Urban Sound Levels." *Environmental Monitoring and Assessment* 187 (1): 4072. <https://doi.org/10.1007/s10661-014-4072-3>.
- Prieto Gajardo, Carlos, Juan Miguel Barrigón Morillas, Guillermo Rey Gozalo, and Rosendo Vílchez-Gómez. 2016. "Can Weekly Noise Levels of Urban Road Traffic, as Predominant Noise Source, Estimate Annual Ones?" *The Journal of the Acoustical Society of America* 140 (5): 3702. <https://doi.org/10.1121/1.4966678>.
- Rey Gozalo, Guillermo, Juan Miguel Barrigón Morillas, and Carlos Prieto Gajardo. 2015. "Urban Noise Functional Stratification for Estimating Average Annual Sound Level." *The Journal of the Acoustical Society of America* 137 (6): 3198–3208. <https://doi.org/10.1121/1.4921283>.
- Segura Garcia, Jaume, Juan Jose Pérez Solano, Máximo Cobos Serrano, Enrique A. Navarro Camba, Santiago Felici Castell, Antonio Soriano Asensi, and Francisco Montes Suay. 2016. "Spatial Statistical Analysis of Urban Noise Data from a WASN Gathered by an IoT System: Application to a Small City." *Applied Sciences* 6 (12): 380. <https://doi.org/10.3390/app6120380>.
- Sevillano, Xavier, Joan Claudi Socoró, Francesc Alías, Patrizia Bellucci, Laura Peruzzi, Simone Radaelli, Paola Coppi, et al. 2016. "DYNAMAP – Development of Low Cost Sensors Networks for Real Time Noise Mapping." *Noise Mapping* 3 (1). <https://doi.org/10.1515/noise-2016-0013>.

- Tilloy, Anne, Vivien Mallet, David Poulet, Céline Pesin, and Fabien Brocheton. 2013. "BLUE-Based NO₂ Data Assimilation at Urban Scale." *Journal of Geophysical Research*, American Geophysical Union, 4 (118): 2031–40.
- Ventura, Raphael, Vivien Mallet, Valerie Issarny, Pierre-Guillaume Raverdy, and Fadwa Rebhi. 2017. "Estimation of Urban Noise with the Assimilation of Observations Crowdsensed by the Mobile Application Ambiciti." In . Hong-Kong.
- Wei, Weigang, Timothy Van Renterghem, Bert De Coensel, and Dick Botteldooren. 2016. "Dynamic Noise Mapping: A Map-Based Interpolation between Noise Measurements with High Temporal Resolution." *Applied Acoustics* 101: 127–40. <https://doi.org/10.1016/j.apacoust.2015.08.005>.
- West, Douglas. 2001. *Introduction to Graph Theory - Second Edition*. 2nd ed. Prentice Hall.
- Zambon, Giovanni, Roberto Benocci, Alessandro Bisceglie, H. Eduardo Roman, and Patrizia Bellucci. 2017. "The LIFE DYNAMAP Project: Towards a Procedure for Dynamic Noise Mapping in Urban Areas." *Applied Acoustics* 124 (September): 52–60. <https://doi.org/10.1016/j.apacoust.2016.10.022>.
- Zuo, Fei, Ye Li, Steven Johnson, James Johnson, Sunil Varughese, Ray Copes, Fuan Liu, Hao Jiang Wu, Rebecca Hou, and Hong Chen. 2014. "Temporal and Spatial Variability of Traffic-Related Noise in the City of Toronto, Canada." *Science of The Total Environment* 472 (Supplement C): 1100–1107. <https://doi.org/10.1016/j.scitotenv.2013.11.138>.